



# Regioselective Isomerization of Terminal Alkenes Catalyzed by a PC( $sp^3$ )Pincer Complex with a Hemilabile Pendant Arm

Sophie De-Botton,<sup>[a]</sup> D.Sc. Oleg A. Filippov,<sup>[b]</sup> Elena S. Shubina,<sup>[b]</sup> Natalia V. Belkova,\*<sup>[b]</sup> and Dmitri Gelman\*<sup>[a, c]</sup>

We describe an efficient protocol for the regioselective isomerization of terminal alkenes employing a previously described bifunctional Ir-based PC( $sp^3$ )complex (**4**) possessing a hemilabile sidearm. The isomerization, catalyzed by **4**, results in a one-step shift of the double bond in good to excellent selectivity, and good yield. Our mechanistic studies revealed that the reaction is driven by the stepwise migratory insertion of Ir–H species

into the terminal double bond/β-H elimination events. However, the selectivity of the reaction is controlled by dissociation of the hemilabile sidearm, which acts as a selector, favoring less sterically hindered substrates such as terminal alkenes; importantly, it prevents recombination and further isomerization of the internal ones.

## Introduction

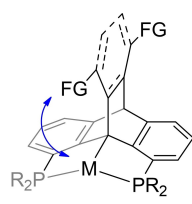
The double bond is one of the most versatile functional groups in organic chemistry because it allows facile and selective manipulation of the molecular skeleton. In general, isomerization of the readily available terminal alkenes into an array of structurally more complex isomers is a useful strategy to create molecular diversity.<sup>[1]</sup> Therefore, changing the position of a double bond in a controllable fashion is a very important tool in organic synthesis, especially for designing one-pot tandem transformations in conjunction with mechanistically related transformations such as hydroformylation, methoxycarbonylation, hydrocyanation, hydroboration, hydrosilylation, olefin metathesis, conjugate additions and many others, affording the synthesis of fine and commodity chemicals, as well as smart utilization of petroleum feedstock (Scheme 1).<sup>[2]</sup>

A wide range of isomerization catalysts have been developed based on transition-metal complexes of such metals as Ir,<sup>[3]</sup> Pd,<sup>[4]</sup> Ru,<sup>[5]</sup> Co,<sup>[6]</sup> Fe,<sup>[7]</sup> Rh,<sup>[8]</sup> Mo,<sup>[9]</sup> Ni,<sup>[10]</sup> and more.<sup>[11]</sup> However, controlling regio- and stereoselectivities in such an isomerization has been a challenge so far because a mixture of positional and geometric isomers is produced during the reaction. Although the site selectivity, controlled thermody-

namically via conjugation to certain functional groups or sterically by skeleton branching, can be achieved, a more general approach would rely on controlling by using a tunable catalyst. For example, one of the more interesting catalyst design principles that have been recently employed to achieve high selectivity and reactivity control relies on the ligand–metal interplay with the aid of a pendant functional group.<sup>[12]</sup>

Our group explores a family of dibenzobarrelene-based pincer ligand systems for various applications in homogeneous catalysis directed toward organic synthesis.<sup>[13]</sup> This ligand class offers a modular, yet structurally and conformationally stable platform for the synthesis of robust C( $sp^3$ )-metatalated compounds<sup>[14]</sup> bearing various functional groups (Figure 1). These functional groups are not innocent in catalysis and are often responsible for secondary catalyst–substrate interactions or even ligand–metal cooperative bond activation.<sup>[15]</sup>

Recently, we demonstrated that the presence of a hemilabile coordinating site in a ligand may lead to a marked change in the organometallic behavior and the catalytic activity of the corresponding transition metal complex, for example, significantly influencing the reactivity of incoming substrates and the rates of elementary reactions.<sup>[16]</sup> For example, our brief comparative studies aiming to identify the reactive species in the transfer dehydrogenation of alkanes demonstrated a significant isomerization of linear alkenes accompanying that major reaction.<sup>[17]</sup>



M = Ni, Pd, Pt, Rh, Ru, Ir  
FG = CO<sub>2</sub>R, OH, NH<sub>2</sub>, CO<sub>2</sub>OH

Figure 1. Previously reported bifunctional C( $sp^3$ )-metatalated compounds.

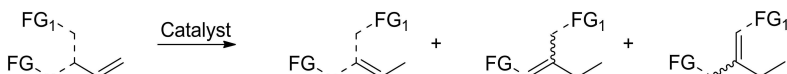
[a] S. De-Botton, Prof. D. Gelman  
Institute of Chemistry, Edmond J. Safra Campus  
The Hebrew University of Jerusalem, Jerusalem, 91904 (Israel)  
E-mail: dmitri.gelman@mail.huji.ac.il

[b] D.S. O. A. Filippov, Prof. E. S. Shubina, Prof. N. V. Belkova  
A.N. Nesmeyanov Institute of Organoelement Compounds  
Russian Academy of Sciences  
Vavilov Street 28, 119991 Moscow (Russia)  
E-mail: nataliabelk@ineos.ac.ru

[c] Prof. D. Gelman  
Peoples' Friendship University of Russia (RUDN University)  
Miklukho-Maklay St., 6, 117198 Moscow (Russia)

 Supporting information for this article is available on the WWW under  
<https://doi.org/10.1002/cetc.202001308>

 This publication is part of a joint Special Collection with EurJIC on "Pincer Chemistry & Catalysis". Please follow the link for more articles in the collection.



Scheme 1. Isomerization of terminal olefins.

Therefore, in this work, we were interested in examining this unwanted transformation in more detail in order to convert it into a useful synthetic method by means of our highly tunable and modular bifunctional catalysts.

## Results and discussion

**Catalysis.** Initial alkene isomerization studies were conducted using five complexes reported by us in the past as catalysts for the transfer dehydrogenation of alkanes.<sup>[17a,b]</sup> Compounds **1–4** possess hemilabile coordinating alkoxy groups: **1–3** are characterized by *mer*-configuration of the PC(*sp*<sup>3</sup>)ligand and a rigid coordination of the sidearm having a different steric bulk complex, whereas **4** is a more flexible analogue with *fac*-coordination of the ligand. Complex **5** was used as a

functionless reference with pincer ligand geometry similar to that of **1–3** (Figure 2).

The initial optimization studies were performed under reaction conditions similar to the transfer dehydrogenation experiments; they comprised 1-octene, 0.5 mol% of catalysts **1–5**, and 1 mol% of *t*-BuONa base in non-polar 1,3,5-mesitylene under high temperature conditions. We decided to stick to these conditions because according to our initial observations, the mechanistically related hydrogen transfer and isomerization are catalyzed by a common species. Under these conditions, high activity was achieved only by the flexible catalyst **4**, which drove the reaction to complete conversion after 24 hours at 120 °C (entries 1–5, Table 1). Interestingly, our attempt to improve the performance of the catalyst by replacing sodium *t*-butoxide with another base (e.g., Cs<sub>2</sub>CO<sub>3</sub>, DBU, LiHMDS, and *i*-Pr<sub>2</sub>NEt) eventually led us to conclude that bases are superfluous for this catalyst and that complete conversions can be achieved under base-free conditions (entry 6, Table 1). Lowering reaction temperatures to 80–100 °C diminished the conversions significantly down to 35–77%, respectively (entries 7–9, Table 1).

Substantial progress was achieved upon screening different solvents. A series of experiments showed that, whereas strongly coordinating solvents, such as acetonitrile or propionitrile, inhibit isomerization at lower temperatures, weakly coordinating solvents, such as DME or THF, accelerate it in comparison with the nonpolar solvents (entries 8–14, Table 1); a reaction in Me–THF led to almost full conversion of 1-octene at 80 °C.

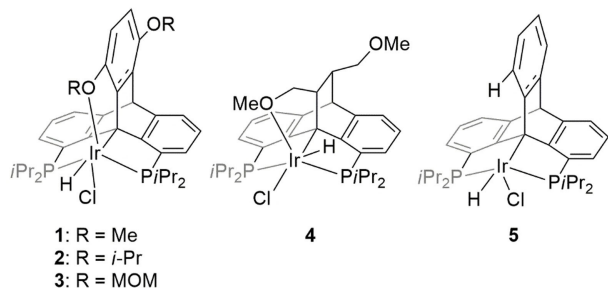
Figure 2. Bifunctional C(*sp*<sup>3</sup>)-metalated compounds used for catalysis.

Table 1. Initial optimization studies.

Entry	Substrate	<i>T</i> [°C]	Solvent	1–5 (0.5%)		<i>t</i> [h]	Conv. [%] <sup>f</sup>
				Cat.	C/S/b <sup>[e]</sup>		
1 <sup>[a]</sup>	1-octene	120	Mesitylene	1	1:200:2	24	8
2 <sup>[a]</sup>	1-octene	120	Mesitylene	2	1:200:2	24	0
3 <sup>[a]</sup>	1-octene	120	Mesitylene	3	1:200:2	24	6
4 <sup>[a]</sup>	1-octene	120	Mesitylene	4	1:200:2	24	>99
5 <sup>[a]</sup>	1-octene	120	Mesitylene	5	1:200:2	24	17
6 <sup>[b]</sup>	1-octene	120	Mesitylene	4	1:200:0	24	>99
7 <sup>[c]</sup>	1-octene	100	Mesitylene	4	1:200:0	24	77
8 <sup>[d]</sup>	1-octene	80	Mesitylene	4	1:200:0	24	35
9 <sup>[d]</sup>	1-octene	80	Benzene	4	1:200:0	24	41
10 <sup>[d]</sup>	1-octene	80	Acetonitrile	4	1:200:0	24	<1
11 <sup>[d]</sup>	1-octene	80	Propionitrile	4	1:200:0	24	<1
12 <sup>[d]</sup>	1-octene	80	DME	4	1:200:0	24	51
13 <sup>[d]</sup>	1-octene	80	THF	4	1:200:0	24	53
14 <sup>[d]</sup>	1-octene	80	Me–THF	4	1:200:0	24	95

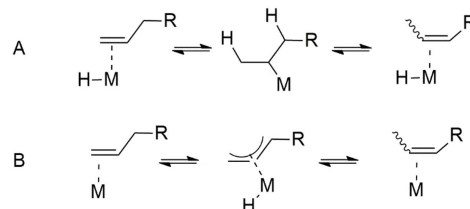
Conditions: [a] Reaction conditions: alkene (0.28 mmol), catalyst **1–5** ( $1.4 \times 10^{-3}$  mmol), base ( $2.8 \times 10^{-3}$  mmol) in 1 mL of mesitylene at 120 °C; [b] Reaction conditions: alkene (0.28 mmol), catalyst **1–5** ( $1.4 \times 10^{-3}$  mmol), no base, in 1 mL of mesitylene at 120 °C; [c] Reaction conditions: alkene (0.28 mmol), catalyst **1–5** ( $1.4 \times 10^{-3}$  mmol), no base, in 1 mL of mesitylene at 100 °C; [d] Reaction conditions: alkene (0.28 mmol), catalyst **1–5** ( $1.4 \times 10^{-3}$  mmol), no base, in 1 mL of different solvents at 80 °C; [e] C/S/b = Catalyst/Substrate/base ratio; [f] Conversion was determined by NMR spectroscopy using internal standard.

With the optimized reaction conditions in hand, the substrate scope for the isomerization was investigated. As shown in Table 2, the isomerization process can be extended to a wide variety of terminal alkenes. All the reactions were carried out using two solvents: (1) Me–THF, since this solvent resulted in the highest rates (*vide supra*), and (2) benzene, since this resulted in the highest selectivity (*vide infra*). Product compositions and stereochemistry were determined by GC or H-NMR. For example, isomerization of allyl benzene was complete after 24 hours of heating at 80 °C in the presence of 0.5 mol% of **4** in MeTHF; there was an excellent E/Z selectivity of 20:1 (entries 1–2, Table 2). The reaction in benzene, however, reached only 74% conversion with the same selectivity. No rate inhibition was observed even with coordinating substrates such as eugenol and complete conversions of the starting material predominantly into the thermodynamically stable *E*-isomer were recorded in both the polar and non-polar media (entries 3–4, Table 2).

However, careful <sup>1</sup>H-NMR analysis of the mixture from a reaction of a longer chain aliphatic substrate, 1-octene, revealed a good regioselectivity for 2-octenes – 58% of 2-octene, although with a relatively low stereoselectivity – *E*/*Z* mixture (2:1) after 61% conversion. Other octene isomers were observed in smaller quantities up to 3% total for 3- and 4-octenes; this corresponds to a ratio of 19:1 between the 2-octene and the higher regioisomers. Interestingly, analysis of the same reaction performed in Me–THF revealed a diminished 5:1 regioselectivity toward 2-octene (2:1 *E*/*Z* ratio), along with other isomers that were present in the reaction mixture after 95% conversion (entries 5–6, Table 2). Similar results have been obtained using longer-chained alkenes, such as 1-dodecane, and functionalized electron-neutral alkenes such as 5-bromopent-1-ene, indicating that the first shift of the double bond is barely reversible in nonpolar benzene and that no other positional isomers are being formed (entries 7–10, Table 2). Employing vinyl cyclohexane as a substrate (entries 11–12, Table 2) showed that isomerization of a terminal double bond to a sterically demanding tri-substituted position is possible, although it proceeds slowly even in Me–THF, resulting in 87% conversion after 24 hours. In benzene only 20% conversion was achieved over the same period of time. However, the double-bond isomerization into the ring was not observed in this case.

This trend was even more pronounced when functionalized alkenes such as methyl-4-pentenoate and 4-pentenoic acid were employed (entries 13–16, Table 2). For these substrates, exclusive formation of the single-step shifted double bonds in benzene versus a 1:1 mixture in Me–THF was observed. The oxygen functionalities of these substrates may chelate and they favour the formation of six-membered metallacycles where the substrate is prearranged to eliminate the kinetic product. However, stronger chelating functional groups, such as amines, slow down or even inhibit the reaction (entries 17–20, Table 2).

**Mechanistic rationale.** Mechanism-wise, alkene isomerization reactions operate either via metal-alkyl or  $\pi$ -allyl intermediates (Scheme 2).<sup>[18]</sup> The metal-alkyl pathway (A) starts with the coordination of the alkene to a transition metal-hydride species, followed by its insertion into the polar M–H bond.<sup>[19]</sup> This

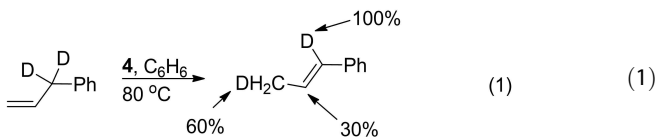


Scheme 2. Isomerization of terminal olefins.

reaction gives two possible metal-alkyl intermediates capable of  $\beta$ -H elimination into either the starting material or its double-bond-shifted isomer upon the regeneration of the reactive catalyst in the form of metal hydride. The  $\pi$ -allyl mechanism (B) involves the oxidative addition of low-valent metal across the allylic C–H bond of the pre-coordinated alkene. The resultant  $\pi$ -allyl complex may reductively eliminate the isomerized product.<sup>[20]</sup>

The virtue of the base-free reaction promoted by catalyst **4** may, in principle, indicate that the reaction takes place via the metal-alkyl pathway because the formation of the low-valent Ir (I) species without base assistance is rather unlikely.<sup>[21]</sup>

Nevertheless, we carried out a stoichiometric H/D scrambling experiment to clarify the mechanism underlying the reaction. A sample of allylbenzene deuterated exclusively in the benzylic position was prepared. Monitoring its isomerization in the presence of stoichiometric **4** in benzene at 80 °C over the course of 12 h by <sup>2</sup>D NMR revealed that the peak corresponding to d<sub>2</sub>-allyl benzene at 3.2 ppm disappeared, and that the product peaks appeared at 6.4, 6.0, and 1.7 ppm in a 1:0.3:0.6 ratio (C1:C2:C3, respectively, Equation 1).



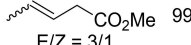
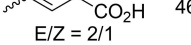
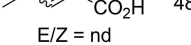
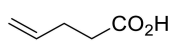
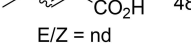
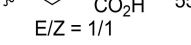
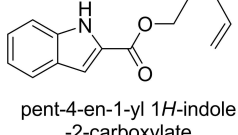
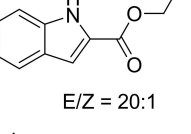
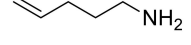
This result was somewhat surprising, because the metal-alkyl pathway either leads to the formation of  $\beta$ -methylstyrene monodeuterated at the  $\alpha$ -position, if the reaction is irreversible, or to the statistical redistribution of the deuterium atoms along the carbon chain, if the reaction is highly reversible.<sup>[22]</sup> Alternatively, under the  $\pi$ -allyl mechanism, no deuteration at C2 is expected.<sup>[23]</sup> The only good explanation for the migration of the D-atom from C1 and its equal distribution between the C2 and C3 positions is that the product-forming stage is essentially irreversible. Here, the Ir–D species, which is expelled at the irreversible stage, participates in the reversible migratory insertion/ $\beta$ -H elimination events that affect only the terminal double bond and, subsequently, only the C2 and C3 positions (Scheme 3).

It is reasonable to assume that the degree of reversibility of the migratory insertion/ $\beta$ -H elimination reactions largely depends on the alkene ability to form a fairly stable complex with the catalyst. As we demonstrated previously, the metal center in **4** is coordinatively and electronically saturated. Therefore,

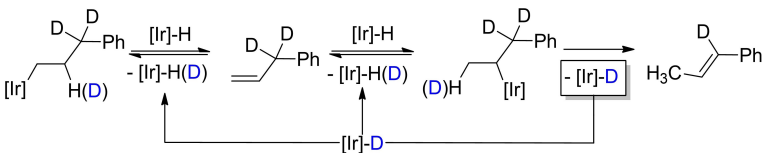
**Table 2.** Scope and limitation studies.

Entry	Substrate	$\xrightarrow[80^\circ\text{C}, 24\text{ h}]{\text{4 (0.5%)}}$	T	Solvent	Conv. [%] <sup>[c]</sup>	Products	
1 <sup>[a]</sup>	Allyl benzene		80 °C	Me–THF	>99		99% E/Z = 20:1
2 <sup>[a]</sup>			80 °C	Benzene	74		74% E/Z = 20:1
3 <sup>[a]</sup>	Eugenol		80 °C	Me–THF	>99		99% E/Z = 19:1
4 <sup>[a]</sup>			80 °C	Benzene	>99		99% E/Z = 17:1
5 <sup>[a]</sup>	1-octene		80 °C	Me–THF	95		76% E/Z = 2/1
							19% E/Z = nd
6 <sup>[a]</sup>			80 °C	Benzene	61		58% E/Z = 2/1
							3% E/Z = nd
7 <sup>[a]</sup>	1-dodecene		80 °C	Me–THF	90		71% E/Z = 2/1
							9% E/Z = nd
8 <sup>[a]</sup>			80 °C	Benzene	62		58% E/Z = 2/1
							4% E/Z = nd
9 <sup>[a]</sup>	5-bromopent-1-ene		80 °C	Me–THF	>99	mixture of compounds	
10 <sup>[b]</sup>			80 °C	Benzene	52		52% E/Z = 2/1
							73%
11 <sup>[a]</sup>	Vinyl cyclohexane		80 °C	Me–THF	87		14%
12 <sup>[a]</sup>			80 °C	Benzene	20		20%
13 <sup>[a]</sup>	Methyl-4-pentenoate		80 °C	Me–THF	>99		49% E/Z = 3/1
							50% E/Z = nd

**Table 2.** continued

Entry	Substrate	T	Solvent	Conv. [%] <sup>[c]</sup>	Products
14 <sup>[a]</sup>		80 °C	Benzene	> 99	 E/Z = 3/1  E/Z = 2/1  E/Z = nd
15 <sup>[a]</sup>		80 °C	Me–THF	94	 E/Z = nd
16 <sup>[a]</sup>	4-pentenoic acid	80 °C	Benzene	55	 E/Z = 1/1
17 <sup>[a]</sup>		80 °C	Me–THF	44	 E/Z = 20:1
18 <sup>[a]</sup>		80 °C	Benzene	5	nd
19 <sup>[a]</sup>		80 °C	Me–THF	< 1	nd
20 <sup>[a]</sup>	pent-4-en-1-amine	80 °C	Benzene	< 1	nd

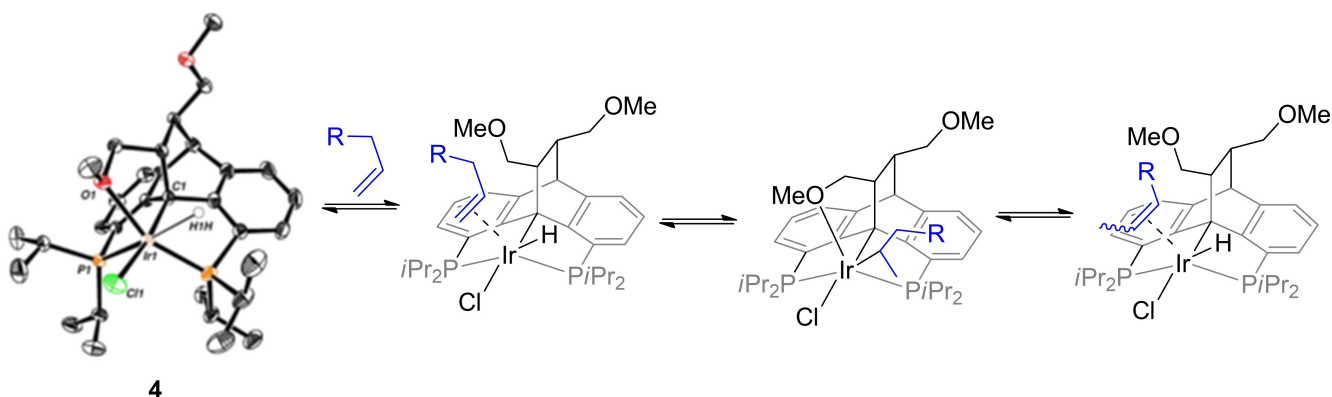
Conditions: [a] alkene (0.28 mmol), catalyst **4** ( $1.4 \times 10^{-3}$  mmol) in 1 mL of Me–THF or benzene at 80 °C; [b] alkene (0.28 mmol), catalyst **4** ( $2.8 \times 10^{-3}$  mmol) in 1 mL of Me–THF or benzene at 80 °C; [c] The yield was determined by NMR spectroscopy using internal standard.

**Scheme 3.** Isomerization of the D-labeled allyl benzene by stoichiometric **4**.

dissociation of the methoxyl group is required for the initial substrate coordination (Scheme 4).

Thus, the hemilabile sidearm acts as a selector favoring the less sterically hindered substrates. This ensures the coordination of the terminal double bonds and prevents recombination and

further isomerization of the internal alkenes, which explains both the isotope labeling experiment as well as the regioselectivity of the reaction toward the one-step isomerization of the terminal alkenes. Indeed, isomerization of *cis*-2-octene by **4** in MeTHF at 80 °C for 24 h resulted in only ca. 25% conversion

**Scheme 4.** Plausible mechanism underlying the alkene isomerization catalyzed by **4**.

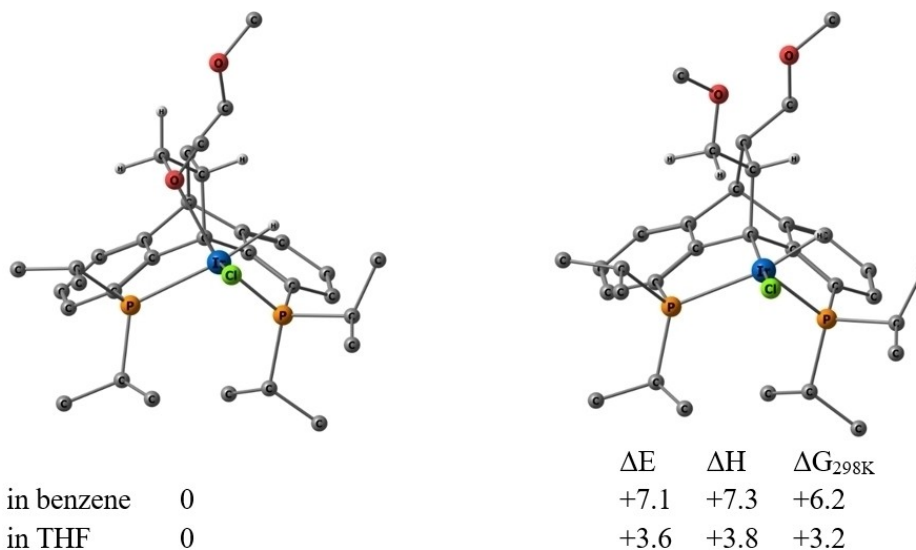


Figure 3. Optimized structures of isomers for complex 4 and their relative energies (in kcal/mol) in benzene and THF.

to 3-octenes versus almost a complete conversion of 1-octene under the same conditions (entry 5, Table 2). The regioselectivity in the isomerization of *cis*-2-octene also matches the results obtained with the terminal alkenes under these conditions.

Finally, to validate the solvent effect, we performed brief DFT calculations aiming at evaluating the dissociation of the MeO-sidearm in THF and benzene. The geometry optimization at the B3PW91/def2-TZVP theory level performed in the corresponding solvent indicated that the dissociation-rotation of the CH<sub>2</sub>OMe group is easier in polar solvents. In THF the species with an open coordination site (Figure 3, right) is only 3 kcal/mol higher than the hexacoordinated isomer. The energy cost of CH<sub>2</sub>OMe group dissociation is twice as large in benzene. The Gibbs free energy difference of two isomers in two solvents suggests that a tenfold higher content of a catalytically active pentacoordinate isomer exists in THF.

It is also reasonable to suggest, that upon CH<sub>2</sub>OMe group dissociation, complex 4 maintains the *fac*-conformation of PC(*sp*<sup>3</sup>)ligand, which is more suitable for alkene insertion into the Ir–H bond. This step is energetically downhill for a *fac*-isomer (please, see ESI).<sup>[24]</sup> Indeed, variable-temperature <sup>1</sup>H and <sup>31</sup>P{<sup>1</sup>H} NMR spectra show only minor signals of the *mer*-isomer even in the presence of 1-octene (see ESI). This may explain the activity of complex 4 surpassing that of other catalysts that feature the *mer*-configuration of PC(*sp*<sup>3</sup>)ligand. The different ratio between 2-alkene and higher regioisomers in the two tested solvents correlates well with the overall conversion of the reactions.

## Conclusions

In conclusion, we studied the isomerization of terminal alkenes catalyzed by a series of iridium complexes possessing PC(*sp*<sup>3</sup>)**1–4** equipped with a hemilabile side-arms. Complex **4**, featuring a more flexible coordination, displayed excellent reactivity and

could induce a selective one-step shift of the terminal double bond in a broad scope of substrates. The reactivity and the regioselectivity of the catalytic isomerization were found to be strongly solvent dependent. Mechanism-wise, the hemilabile sidearm acts as a selector favoring the less sterically hindered substrates, which favors the coordination of terminal double bonds and prevents recombination and further isomerization of the internal ones. However, the most important conclusion from this work is that the unique topology of this family of compounds and flexibility in their synthesis offer nearly unlimited opportunities for the fine-tuning of the catalytic activity in many classical reaction schemes, as well as render new reactivities to many classical organometallic catalysts.

## Acknowledgments

This research was supported by the ISF (Israel Science Foundation) Grant Nos. 917/15, the RUDN University Program "5-100" and by the Esther K. and M. Mark Watkins Chair for Synthetic Organic Chemistry. The DFT calculations and spectroscopic studies were supported by the Russian Science Foundation (grant № 19-13-00459). The use of the equipment of the Center for molecular composition studies of INEOS RAS supported by the Ministry of Science and Higher Education of the Russian Federation is gratefully acknowledged. The authors declare no competing financial interests.

## Conflict of Interest

The authors declare no conflict of interest.

**Keywords:** pincer complexes · ligand-metal cooperation · isomerization · alkenes

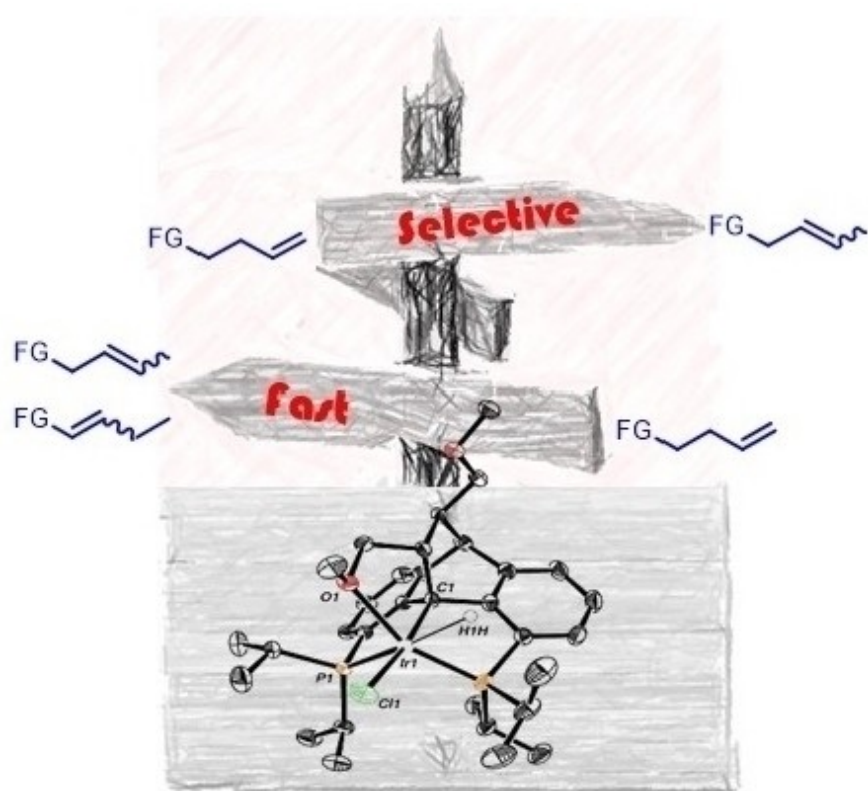
- [1] a) A. Vasseur, J. Bruffaerts, I. Marek, *Nat. Chem.* **2016**, *8*, 209–219; b) J. J. Molloy, T. Morack, R. Gilmour, *Angew. Chem. Int. Ed.* **2019**, *58*, 13654–13664; c) X. Liu, B. Li, Q. Liu, *Synthesis* **2019**, *51*, 1293–1310; d) S. Krompiec, M. Krompiec, R. Penczek, H. Ignasiak, *Coord. Chem. Rev.* **2008**, *252*, 1819–1841; e) N. Kuznik, S. Krompiec, *Coord. Chem. Rev.* **2007**, *251*, 222–233; f) G. Hilt, *ChemCatChem* **2014**, *6*, 2484–2485.
- [2] a) M. Vilches-Herrera, L. Domke, A. Boerner, *ACS Catal.* **2014**, *4*, 1706–1724; b) M. Liniger, Y. Liu, B. M. Stoltz, *J. Am. Chem. Soc.* **2017**, *139*, 13944–13949; c) X. Du, Z. Huang, *ACS Catal.* **2017**, *7*, 1227–1243; d) M. C. Haibach, S. Kundu, M. Brookhart, A. S. Goldman, *Acc. Chem. Res.* **2012**, *45*, 947–958; e) P. Kathe, I. Fleischer, *ChemCatChem* **2019**, *11*, 3343–3354; f) J. Pollini, W. M. Pankau, L. J. Goossen, *Chem. Eur. J.* **2019**, *25*, 7416–7425; g) C. M. Macaulay, S. J. Gustafson, J. T. Fuller, D.-H. Kwon, T. Ogawa, M. J. Ferguson, R. McDonald, M. D. Lumsden, S. M. Bischof, O. L. Sydora, D. H. Ess, M. Stradiotto, L. Turcule, *ACS Catal.* **2018**, *8*, 9907–9925; h) G. E. Dobereiner, G. Erdogan, C. R. Larsen, D. B. Grotjahn, R. R. Schrock, *ACS Catal.* **2014**, *4*, 3069–3076; i) Y. Fujii, T. Takehara, T. Suzuki, H. Fujioka, S. Shuto, M. Arisawa, *Adv. Synth. Catal.* **2015**, *357*, 4055–4062; j) Y. Yuki, K. Takahashi, Y. Tanaka, K. Nozaki, *J. Am. Chem. Soc.* **2013**, *135*, 17393–17400; k) E. Ploshnik, K. M. Langner, A. Halevi, M. Ben-Lulu, A. H. E. Mueller, J. G. E. M. Fraaije, G. J. Agur Sevink, R. Shenhar, *Adv. Funct. Mater.* **2013**, *23*, 4215–4226.
- [3] a) A. R. Chianese, S. E. Shaner, J. A. Tendler, D. M. Pudalov, D. Y. Shopov, D. Kim, S. L. Rogers, A. Mo, *Organometallics* **2012**, *31*, 7359–7367; b) Y. Ebe, M. Onoda, T. Nishimura, H. Yorimitsu, *Angew. Chem. Int. Ed.* **2017**, *56*, 5607–5611; *Angew. Chem.* **2017**, *129*, 5699–5703; c) A. Kumar, T. Zhou, T. J. Emge, O. Mironov, R. J. Saxton, K. Krogh-Jespersen, A. S. Goldman, *J. Am. Chem. Soc.* **2015**, *137*, 9894–9911; d) I. Massad, H. Sommer, I. Marek, *Angew. Chem. Int. Ed.* **2020**, *10*, 7154–7161; e) K. Singh, S. J. Staig, J. D. Weaver, *J. Am. Chem. Soc.* **2014**, *136*, 5275–5278.
- [4] a) L. Lin, C. Romano, C. Mazet, *J. Am. Chem. Soc.* **2016**, *138*, 10344–10350; b) J. Liu, C. Jacob, K. J. Sheridan, F. Al-Mosule, B. T. Heaton, J. A. Iggo, M. Matthews, J. Pelletier, R. Whyman, J. F. Bickley, A. Steiner, *Dalton Trans.* **2010**, *39*, 7921–7935; c) A. L. Kocen, M. Brookhart, O. Daugulis, *Chem. Commun.* **2017**, *53*, 10010–10013; d) A. L. Kocen, K. Klimovica, M. Brookhart, O. Daugulis, *Organometallics* **2017**, *36*, 787–790; e) M. Navarro, V. Rosar, T. Montini, B. Milani, M. Albrecht, *Organometallics* **2018**, *37*, 3619–3630; f) W. Ren, F. Sun, J. Chu, Y. Shi, *Org. Lett.* **2020**, *22*, 1868–1873; g) Y. Yamasaki, T. Kumagai, S. Kanno, F. Kakiuchi, T. Kochi, *J. Org. Chem.* **2018**, *83*, 9322–9333.
- [5] a) Z. Lv, Z. Chen, Y. Hu, W. Zheng, H. Wang, W. Mo, G. Yin, *ChemCatChem* **2017**, *9*, 3849–3859; b) E. R. Paulson, E. Delgado, A. L. Cooksy, D. B. Grotjahn, *Org. Process Res. Dev.* **2018**, *22*, 1672–1682; c) Z. Yang, B. Zhang, G. Zhao, J. Yang, X. Xie, X. She, *Org. Lett.* **2011**, *13*, 5916–5919; d) N. J. Beach, J. M. Blacquiere, S. D. Drouin, D. E. Fogg, *Organometallics* **2009**, *28*, 441–447; e) C. R. Larsen, G. Erdogan, D. B. Grotjahn, *J. Am. Chem. Soc.* **2014**, *136*, 1226–1229; f) E. R. Paulson, C. E. Moore, A. L. Rheingold, D. P. Pullman, R. W. Sindewald, A. L. Cooksy, D. B. Grotjahn, *ACS Catal.* **2019**, *9*, 7217–7231; g) A. V. Smarun, F. Duzhin, M. Petkovic, D. Vidovic, *Dalton Trans.* **2017**, *46*, 14244–14250; h) J. A. Wiles, C. E. Lee, R. McDonald, S. H. Bergens, *Organometallics* **1996**, *15*, 3782–3784.
- [6] a) X. Liu, W. Zhang, Y. Wang, Z.-X. Zhang, L. Jiao, Q. Liu, *J. Am. Chem. Soc.* **2018**, *140*, 6873–6882; b) H. Liu, C. Cai, Y. Ding, J. Chen, B. Liu, Y. Xia, *ACS Omega* **2020**, *5*, 11655–11670; c) J. Zhao, B. Cheng, C. Chen, Z. Lu, *Org. Lett.* **2020**, *22*, 837–841; d) A. Schmidt, A. R. Noedling, G. Hilt, *Angew. Chem. Int. Ed.* **2015**, *54*, 801–804; *Angew. Chem.* **2015**, *127*, 814–818; e) T. Kobayashi, H. Yorimitsu, K. Oshima, *Chem. Asian J.* **2009**, *4*, 1078–1083; f) C. Chen, T. R. Dugan, W. W. Brennessel, D. J. Weix, P. L. Holland, *J. Am. Chem. Soc.* **2014**, *136*, 945–955.
- [7] a) T. Xia, Z. Wei, B. Spiegelberg, H. Jiao, S. Hinze, J. G. de Vries, *Chem. Eur. J.* **2018**, *24*, 4043–4049; b) R. Jennerjahn, R. Jackstell, I. Piras, R. Franke, H. Jiao, M. Bauer, M. Beller, *ChemSusChem* **2012**, *5*, 734–739; c) M. Mayer, A. Welther, A. J. von Wangelin, *ChemCatChem* **2011**, *3*, 1567–1571; d) K. R. Sawyer, E. A. Glascoe, J. F. Cahoon, J. P. Schlegel, C. B. Harris, *Organometallics* **2008**, *27*, 4370–4379.
- [8] a) B. B. Sarma, J. Kim, J. Amsler, G. Agostini, C. Weidenthaler, N. Pfaender, R. Arenal, P. Concepcion, P. Plessow, F. Studt, G. Prieto, *Angew. Chem. Int. Ed.* **2020**, *59*, 5806–5815; b) L.-G. Zhuo, Z.-K. Yao, Z.-X. Yu, *Org. Lett.* **2013**, *15*, 4634–4637; c) S. Y. Y. Yip, C. Aissa, *Angew. Chem. Int. Ed.* **2015**, *54*, 6870–6873; *Angew. Chem.* **2015**, *127*, 6974–6977; d) H. Schumann, O. Stenzel, S. Dechert, F. Girsdis, J. Blum, D. Gelman, R. L. Halterman, *Eur. J. Inorg. Chem.* **2002**, *1*, 211–219.
- [9] a) J. Becica, O. D. Glaze, D. I. Wozniak, G. E. Dobereiner, *Organometallics* **2018**, *37*, 482–490; b) R. Castro-Rodrigo, S. Chakraborty, L. Munjanja, W. W. Brennessel, W. D. Jones, *Organometallics* **2016**, *35*, 3124–3131.
- [10] a) S. Gao, J. Chen, M. Chen, *Chem. Sci.* **2019**, *10*, 3637–3642; b) F. Weber, A. Schmidt, P. Roese, M. Fischer, O. Burghaus, G. Hilt, *Org. Lett.* **2015**, *17*, 2952–2955; c) Q. Wu, L. Wang, R. Jin, C. Kang, Z. Bian, Z. Du, X. Ma, H. Guo, L. Gao, *Eur. J. Org. Chem.* **2016**, *2016*, 5415–5422; d) J. Breitenfeld, O. Vechorkin, C. Corminboeuf, R. Scopelliti, X. Hu, *Organometallics* **2010**, *29*, 3686–3689; e) J. Blum, D. Gelman, Z. Aizenshtat, S. Wernik, H. Schumann, *Tetrahedron Lett.* **1998**, *39*, 5611–5614.
- [11] M. K. Leclerc, H. H. Brintzinger, *J. Am. Chem. Soc.* **1996**, *118*, 9024–9032.
- [12] a) Y. Wang, C. Qin, X. Jia, X. Leng, Z. Huang, *Angew. Chem. Int. Ed.* **2017**, *56*, 1614–1618; *Angew. Chem.* **2017**, *129*, 1636–1640; b) M. R. Kita, A. J. M. Miller, *Angew. Chem. Int. Ed.* **2017**, *56*, 5498–5502; *Angew. Chem.* **2017**, *129*, 5590–5594.
- [13] a) C. Azerraf, D. Gelman, *Chem. Eur. J.* **2008**, *14*, 10364–10368; b) C. Azerraf, D. Gelman, *Organometallics* **2009**, *28*, 6578–6584; c) C. Azerraf, A. Shpruhman, D. Gelman, *Chem. Commun.* **2009**, *4*, 466–468; d) S. Musa, A. Shpruhman, D. Gelman, *J. Organomet. Chem.* **2012**, *699*, 92–95; e) O. Cohen, O. Grossman, L. Vaccaro, D. Gelman, *J. Organomet. Chem.* **2014**, *750*, 13–16; f) L. Kaganovsky, K.-B. Cho, D. Gelman, *Organometallics* **2008**, *27*, 5139–5145.
- [14] a) D. Gelman, R. Romm, *Top. Organomet. Chem.* **2013**, *40*, 289–318; b) C. Azerraf, S. Cohen, D. Gelman, *Inorg. Chem.* **2006**, *45*, 7010–7017; c) C. Azerraf, O. Grossman, D. Gelman, *J. Organomet. Chem.* **2007**, *692*, 761–767; d) I. Kisets, D. Gelman, *Organometallics* **2018**, *37*, 526–529; e) A. Singh, D. Gelman, *ACS Catal.* **2020**, *10*, 1246–1255.
- [15] a) S. Musa, R. Romm, C. Azerraf, S. Koizuchi, D. Gelman, *Dalton Trans.* **2011**, *40*, 8760–8763; b) S. Musa, I. Shaposhnikov, S. Cohen, D. Gelman, *Angew. Chem. Int. Ed.* **2011**, *50*, 3533–3537; *Angew. Chem.* **2011**, *123*, 3595–3599; c) D. Gelman, S. Musa, *ACS Catal.* **2012**, *2*, 2456–2466; d) G. A. Silantyev, O. A. Filippov, S. Musa, D. Gelman, N. V. Belkova, K. Weisz, L. M. Epstein, E. S. Shubina, *Organometallics* **2014**, *33*, 5964–5973; e) S. Musa, A. Ghosh, L. Vaccaro, L. Ackermann, D. Gelman, *Adv. Synth. Catal.* **2015**, *357*, 2351–2357; f) V. A. Kirkina, E. S. Osipova, O. A. Filippov, G. A. Silantyev, D. Gelman, E. S. Shubina, N. V. Belkova, *Mendeleev Commun.* **2020**, *30*, 276–278.
- [16] a) S. Cohen, A. N. Bilyachenko, D. Gelman, *Eur. J. Inorg. Chem.* **2019**, *19*, 3203–3209; b) S. Mujahed, F. Valentini, S. Cohen, L. Vaccaro, D. Gelman, *ChemSusChem* **2019**, *12*, 4693–4699.
- [17] a) S. De-Botton, S. Cohen, D. Gelman, *Organometallics* **2018**, *37*, 1324–1330; b) V. A. Kirkina, G. A. Silantyev, S. De-Botton, O. A. Filippov, E. M. Titova, A. A. Pavlov, N. V. Belkova, L. M. Epstein, D. Gelman, E. S. Shubina, *Inorg. Chem.* **2020**, *59*, 11962–11975; c) S. De-Botton, R. Romm, G. Bensoussan, M. Hitrik, S. Musa, D. Gelman, *Dalton Trans.* **2016**, *45*, 16040–16046.
- [18] W. A. Herrmann, M. Prinz, Vol. 3, Wiley-VCH Verlag GmbH, 2002, pp. 1119–1130.
- [19] a) E. Larionov, H. Li, C. Mazet, *Chem. Commun.* **2014**, *50*, 9816–9826; b) S. M. M. Knapp, S. E. Shaner, D. Kim, D. Y. Shopov, J. A. Tendler, D. M. Pudalov, A. R. Chianese, *Organometallics* **2014**, *33*, 473–484; c) V. S. Petrosyan, A. B. Permin, V. I. Bogdashkina, D. P. Krut'ko, *J. Organomet. Chem.* **1985**, *292*, 303–309.
- [20] a) I. Massad, I. Marek, *ACS Catal.* **2020**, *10*, 5793–5804; b) K. Tani, *Pure Appl. Chem.* **1985**, *57*, 1845–1854.
- [21] V. V. Grushin, *Acc. Chem. Res.* **1993**, *26*, 279–286.
- [22] a) S. Biswas, *Comments Inorg. Chem.* **2015**, *35*, 300–330; b) D. V. McGrath, R. H. Grubbs, *Organometallics* **1994**, *13*, 224–235; c) F. C. Courchay, J. C. Sworen, I. Ghiviriga, K. A. Abboud, K. B. Wagener, *Organometallics* **2006**, *25*, 6074–6086.
- [23] S. Biswas, Z. Huang, Y. Cholli, D. Y. Wang, M. Brookhart, K. Krogh-Jespersen, A. S. Goldman, *J. Am. Chem. Soc.* **2012**, *134*, 13276–13295.
- [24] S. Musa, O. A. Filippov, N. V. Belkova, E. S. Shubina, G. A. Silantyev, L. Ackermann, D. Gelman, *Chem. Eur. J.* **2013**, *19*, 16906–16909.

Manuscript received: August 11, 2020

Revised manuscript received: September 7, 2020

Accepted manuscript online: September 8, 2020

Version of record online: ■■■



S. De-Botton, D.S. O. A. Filippov,  
Prof. E. S. Shubina, Prof. N. V.  
Belkova\*, Prof. D. Gelman\*

1 – 8

Regioselective Isomerization of  
Terminal Alkenes Catalyzed by a  
PC( $sp^3$ )Pincer Complex with a  
Hemilabile Pendant Arm



**Bifunctional pincer complexes:** We describe an efficient protocol for the divergent regioselective isomerization

of terminal alkenes employing a bi-functional Ir-based PC( $sp^3$ ) complex possessing a hemilabile sidearm.